

See discussions, stats, and author profiles for this publication at: <https://www.researchgate.net/publication/363114503>

The emerging pathogen *Enterocytozoon hepatopenaei* drives a degenerative cyclic pattern in the hepatopancreas microbiome of the shrimp (*Penaeus vannamei*)

Article in *Scientific Reports* · August 2022

DOI: 10.1038/s41598-022-19127-2

CITATIONS

0

3 authors:



Antonio López Carvallo

Ensenada Center for Scientific Research and Higher Education

19 PUBLICATIONS 65 CITATIONS

[SEE PROFILE](#)

READS

161



Roberto Cruz-Flores

Ensenada Center for Scientific Research and Higher Education

40 PUBLICATIONS 255 CITATIONS

[SEE PROFILE](#)



Arun K. Dhar

The University of Arizona

124 PUBLICATIONS 2,714 CITATIONS

[SEE PROFILE](#)

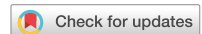
Some of the authors of this publication are also working on these related projects:



Characterization of regulatory elements of viruses [View project](#)



Whole genome reconstruction of pathogens of aquatic organisms from archived Davidson's-fixed paraffin embedded tissues [View project](#)



OPEN

The emerging pathogen *Enterocytozoon hepatopenaei* drives a degenerative cyclic pattern in the hepatopancreas microbiome of the shrimp (*Penaeus vannamei*)

Jesús Antonio López-Carvallo ¹, Roberto Cruz-Flores ^{1,2} & Arun K. Dhar ²✉

The microsporidian *Enterocytozoon hepatopenaei* (EHP) is an emerging pathogen that causes substantial economic losses in shrimp (*Penaeus* spp.) aquaculture worldwide. To prevent diseases in shrimp, the manipulation of the gut microbiota has been suggested. However, prior knowledge of the host-microbiome is necessary. We assessed the modulation of the microbiome (bacteria/fungi) and its predicted functions over the course of disease progression in shrimp experimentally challenged with EHP for 30 days using high throughput 16S rRNA and ITS amplicon sequencing. Infection grade was assessed for the first time by quantitative digital histopathology. According to the infection intensity, three disease-stages (early/developmental/late) were registered. During the early-stage, EHP was not consistently detected, and a high diversity of potentially beneficial microorganisms related to nutrient assimilation were found. In the development-stage, most of the shrimp start to register a high infection intensity related to a decrease in beneficial microorganisms and an increase in opportunistic/pathogenic fungi. During late-stage, animals displayed different infection intensities, showed a displacement of beneficial microorganisms by opportunistic/pathogenic bacteria and fungi related to pathogen infection processes and depletion of energetic reserves. The degenerative cyclic pattern of EHP infection and its effects on beneficial microorganisms and beneficial functions of the shrimp hepatopancreas microbiome are discussed.

The white leg shrimp, *Penaeus vannamei*, is an economically important species that represents 52.9% of the total production of crustacean aquaculture (9.4 million tons) worldwide¹. Even though production has been steadily increasing in recent years, shrimp aquaculture is in constant challenge for the emergence and spread of new diseases such as hepatopancreatic microsporidiosis (HPM) caused by an emergent pathogen *Enterocytozoon hepatopenaei* (EHP). This disease was first reported in 2001, affecting black tiger shrimp *P. monodon* and was tentatively termed monodon slow growth syndrome (MSGs)². In 2009, EHP was formally described from *P. monodon*³ postlarvae/juveniles and the disease was later referred as HPM⁴.

Hepatopancreatic microsporidiosis has now been reported in Thailand, Vietnam, India, China, Indonesia, Malaysia, Venezuela and has kept spreading to other countries where shrimp culture takes place⁵. Presently, EHP is considered one of the major threats to shrimp culture⁶ and is imposing major limitations to shrimp farming across Asia^{5,7}. Since sanitary measures around the world have historically failed to contain the spread of pathogens in shrimp farming⁸ and only a few functional therapeutic methods are available to treat crustacean diseases⁹, researchers have focused their efforts on exploring novel alternatives to prevent diseases in shrimp including the modulation of the host-microbiome^{10,11}. The last is a promising alternative as the microbiome is closely related to particular functions of the host^{11–13} and can be used as a driver for success in shrimp farming¹⁰, which may help to prevent/control EHP infection.

The modulation of the microbiome has been used to improve shrimp health, growth performance and resistance to disease which in turn favors higher farm production¹⁴. This modulation can be attained at a farm level in

¹Centro de Investigación Científica y de Educación Superior de Ensenada (CICESE), Carretera Ensenada-Tijuana No. 3918, Zona Playitas, 22860 Ensenada, Baja CA, Mexico. ²Aquaculture Pathology Laboratory, School of Animal and Comparative Biomedical Sciences, The University of Arizona, 1117 Lowell Street, Tucson, AZ 85721, USA. ✉email: adhar@arizona.edu

shrimp culture by using probiotics, prebiotics, symbiotics, and by creating an environment favorable to probiotics (e.g. biofloc)^{14,15}. However, to modulate the microbiome in a beneficial manner that promotes increased growth requires prior knowledge of health and diseased shrimp microbiomes¹⁰.

The microbiome status of an organism can be deciphered by using new generation technologies such as high throughput sequencing through the amplification and sequencing of the hypervariable regions of genes such as 16S rRNA for bacteria and internal transcribed spacer (ITS) for fungi¹⁶. Amplicon sequencing by high throughput methods allows the quantification of microorganisms' taxa abundance, assess microbial diversity and predicts the microbiome functions based on the prevalent microorganisms' taxa¹⁷. These methods have been used by many researchers to obtain a high-resolution map of the host-microbiome¹⁰. Furthermore, they allow a better insight into the complex interactions between host and microorganisms when the health condition are affected by the presence of pathogens¹⁰.

Insights on the modulation of the hepatopancreatic microbiota (bacteria and fungi) and associated functions by EHP in *P. vannamei* are greatly lacking. This study evaluated the composition, diversity and functions of hepatopancreas microbiota of the pacific white shrimp *P. vannamei* infected with EHP for 30 days following a pathogen challenge. The findings greatly enhanced our understanding of disease stage-specific community assembly patterns in the shrimp hepatopancreas micro-ecosystem upon infection with EHP.

Methods

Shrimp acquisition. Specific pathogen-free (SPF) shrimp, *P. vannamei* (~5 g) originating in the Oceanic Institute (Oahu, Hawaii, USA) were used for the experimental bioassay conducted in the Aquaculture Pathology Laboratory of the University of Arizona. All animals used in this study are certified SPF and these stocks have consistently tested negative for the OIE-listed and the OIE non-listed pathogens including EHP. Before the experiment shrimp were acclimatized for 2 weeks in a 100 L recirculating culture system (25 °C) provided with gentle aeration and fed with a commercial shrimp diet (Rangen, 40% protein).

Experimental challenge. Experimental challenge was conducted following a cohabitation challenge method. Briefly, upon acclimatization, animals were tagged by cutting a small piece of the uropod to identify challenged SPF shrimp from the EHP-infected population. Before SPF *P. vannamei* were exposed to EHP-infected shrimp (day 0), a total of two SPF shrimp were sampled and hepatopancreas tissue was aseptically excised, one part was flash-frozen in liquid nitrogen and the other section was fixed in Davison alcohol-formalin-acetic acid (AFA) solution. On the following day, a total of 36 SPF shrimp were transferred to an experimental tank that held known EHP-infected *P. vannamei* shrimp. The cohabitation challenge was conducted for 30 days while experimental animals were sampled throughout the challenge period. Transmission of EHP by co-habitation was preferred as it is a fast and cost-effective method for parasite propagation that closely simulates natural routes of EHP infection in a shrimp farm^{18,19}.

During the experimental challenge, the organisms were fed daily a commercially pellet shrimp diet (Rangen, 40% protein) for the duration of the study, and temperature and salinity in the tank were held to 25 °C and 33 parts per unit, respectively. Through the entire duration of the challenge experiment, on every third day two (third and sixth day) to three (from the ninth day onwards) tagged SPF shrimp were sampled. The hepatopancreas was excised into two equal parts of tissue, one part was flash-frozen and kept at -80 °C for microbiome analysis, and the other one was fixed in Davidson AFA solution for in situ hybridization analysis. The hepatopancreas tissue was selected as a target tissue since EHP develops and replicates in this tissue³. This study was performed following standard protocols of the University of Arizona-Aquaculture Pathology Laboratory which is an USDA and ISO (17043 and 170225) accredited laboratory for Crustacean Disease Diagnosis.

Quantitative digital histopathology using in situ hybridization. As a strategy to evaluate the infection grade of the cohabitation challenged shrimp, a quantitative digital histopathology analysis was performed. In situ hybridization (ISH) was performed following methodologies previously reported to detect EHP²⁰ where EHP-specific primers 510 F (5'-GCCTGA GAG ATG GCT CCC ACG T-3') and 510 R (5'-GCG TAC TAT CCC CAG AGC CCG A-3') are used and tailed with digoxigenin-11-dUTP (Integrated DNA Technologies, San Diego, CA, USA) at 3' end. The severity of EHP infection was graded from G0–G4 following a semi-quantitative grading scheme²¹. Briefly, Grade 0 indicates no signs of infection, Grade 1 indicates signs of infection by the pathogen but at levels that may be below to those needed for clinical disease, Grade 2 moderate signs of infection shown by number and severity of pathogen caused lesions, Grade 3 moderate to high signs of disease shown by number and severity of pathogen caused lesions and Grade 4 high numbers of pathogen caused lesions and tissue destruction.

The ISH glass slides that contained the dissected tissue area were scanned and digitalized using a MoticEasy-Scan Pro 6 Pathology Slide Scanner (Meyer Instruments, Inc., TX, USA). Digital images were processed with Image-Pro Plus 10.0 (Media Cybernetics, Bethesda, MD, USA) according to López-Carvallo et al.²². In each slide, three random images at 10× magnification were selected considering the infected areas as representative of the infection of that particular shrimp. This information was used to calculate the EHP infection index (EII) using the following formula: EII (%) = ((CAE/TCA) × 100), where CAE is the coverage area of EHP (μm^2), and TCA is the total coverage area of the analyzed region of the affected tissue (μm^2). A range of EII percentages was assigned to the severity of the infection grade scale proposed by Lightner²¹. The EII percentages were normalized by arcsin, and a one-way analysis of variance was performed to assess significant differences as a function of infection grade and stage of the disease.

Bacterial and fungal DNA isolation. A total of 30 flash-frozen samples of hepatopancreas from tagged SPF shrimp that were kept in cohabitation with EHP infected shrimp were used to extract bacterial and fungal genomic DNA (gDNA) from each animal. The total gDNA was extracted from the sampled tissue (20 mg) using the Genomic DNA Isolation Kit (Norgen Biotek Corp[®], ON, Canada) and the Maxwell[®] 16 Cell LEV DNA Purification Kit (Promega, WI, USA) according to the manufacturer's instructions.

The integrity of total gDNA was corroborated by gel electrophoresis, and quality and concentration were measured by a NanoDrop 2000/2000c[™] (Thermo Fisher Scientific, Waltham, MA, USA). The isolated DNA were sent for NGS at OmegaBioservices, Norcross, GA. PCR reactions were performed using 16S rRNA primers IlluminaF (5'-CCTACGGGNNGCWGCAG-3') and IlluminaR (5'-ACTACHVGGGTATC-TAATCC-3') while the internal transcribed spacer (ITS) was amplified using the primers ITS1F (5'-C TTG GTC ATT TAG AGG AAG TAA-3') and ITS4R (5'-T CCT CCG CTT ATT GAT ATG C-3').

16S rRNA V3-V4 and ITS amplicons sequencing. Before construction of the libraries, gDNA quality was assessed using TapeStation (Agilent[®]). A total of 30 libraries for bacteria analysis and 30 libraries for fungal analysis were prepared using the kit KAPA HyperPlus (Roche[®], Basile, Switzerland) according to the manufacturer's recommendations. Library quality was analyzed with Agilent Bioanalyzer 2100 system (Agilent[®], Santa Clara, CA, USA) and sequenced with Illumina Mi-Seq[®] platform (San Diego, CA, USA) on mode pair-end (2X300). The generation of libraries and sequencing was performed by OmegaBioservices (Norcross, GA, USA). A total of 1,331,020 16S rRNA V3–V4 and 883,460 ITS raw reads were generated via sequencing.

Bioinformatics and statistical analysis. To increase the number of runs using different parameters to evaluate the microbiome of *P. vannamei* infected with EHP, we decided to use a graphical user interface tool called EasyMAP¹⁷. This tool integrates Quantitative Insights Into Microbial Ecology 2 (QIIME2, 2018.4.0 version)²³, Linear Discriminant Analysis Effect Size (LefSe, 1.0.8.post1 version)²⁴, and Phylogenetic Investigation of Communities by Reconstruction of Unobserved States (PICRUSt, 1.1.3 version)²⁵ pipelines, and incorporates the database of Greengenes, SILVA and UNITE¹⁷. Databases generated from high through sequencing for bacterial and fungal analysis were analyzed separately using the same pipeline except for the database. Greengenes Database was used to identify the bacterial taxa and UNITE to identify the fungus taxa. The raw reads were first analyzed with the FastQC software²⁶ to assess the quality. The pair-end libraries containing raw read, sample metadata and manifest files were uploaded at the EasyMAP portal (<http://easymap.cgm.ntu.edu.tw/>). These files are used to identify libraries and define the statistical group for each sample for later analysis¹⁷.

For all statistical analyses, we used three groups according to the disease stage classification (early, development and late), where individual organisms were considered as biological replicates. This decision was made according to multiple clustering analyses since it has been confirmed that organisms clustered in the same group are related to similar physiological conditions, tissue or environment^{27,28}. Pearson's correlation and PCoA mainly sustain the clustering by disease-stage compared to infection grade and time of exposure with the pathogen.

Since sequence files were already demultiplexed, the manifest file was used according to the EasyMAP platform¹⁷. QIIME2 plug-in q2-dada2 was used to trimmed low-quality read ($Q < 25$), merge pair-end high-quality reads and remove chimeric sequences. No chimeric sequences were used for operational taxonomic unit (OTU) assignment. The taxonomic analysis (OUT table construction, taxonomy assignment, relative abundances tables by taxa) was assessed using the QIIME2 plug-in q2-feature-classifier. A 97% of sequence similarity was considered for sequence clustering and similar sequences from the same taxa were clustered into one OTU. The phylogenetic tree generation was performed by the plug-in q2-alignment and q2-phylogeny. Frequency bars graphs for phyla and Heatmaps for genera visualization were plotted in R.

The taxonomy differential abundance analysis was performed by the LefSe plug-in using the KEGG database at level three and Wilcoxon test ($\alpha < 0.05$). Taxonomy differential abundance was only registered when $LDA > 2$. Taxa abundance that were differentially expressed was plotted using bar, heatmap and circular cladogram graphics provided by EasyMAP platform or plotted using R.

The platform EasyMAP provided statistical results for alpha and beta diversity. Observed OTUs, Shannon diversity index (H) and Simpson's diversity index (D) were used as standard statistical tools of alpha diversity and Principal Coordinates Analysis (PCoA) for beta diversity analysis. Alpha diversity was assessed by Kruskal-Wallis of all groups and pair-wise; ($P < 0.05$) and visualized using box plots. The beta diversity was assessed by PERMANOVA ($P < 0.05$) using Jaccard methodology (measures presence/absence) and PCoA was used to visualize microorganism composition and abundance similarity/dissimilarity between samples.

Microbiome function was predicted by using taxa abundance differentially expressed and the PICRUSt plug-in which mapped Greengenes IDs to the corresponding KEGG pathway. This tool has been used to predict the bacterial functional composition in crustaceans' guts²⁹. The predicted microbiome function was plotted by circular graphics using a log10 LDA score.

The heatmaps, bar, and circular graphs, and hierarchical clustering (Pearson correlation) were performed by using ggplot2 and hclust, respectively, using R software in Rstudio³⁰. Relative abundance shown in heatmaps figures were log2 transformed to visualize taxa with low relative abundance (< 1%). The general experimental design can be visualized as a graphical abstract to aid readers' comprehension (Fig. 1). For all replicates, a descriptive ID was added including sample day (D0–D30), infection grade (I0–I4), and the replicate number (R1–R3) to facilitate tracking of the microbiome changes caused by EHP infection (e.g. D0_I0_R1). In addition, the statistical groups (disease stages) were marked in three different colors (Early: green; Development: red; Late: blue) for bacteria and fungi analyses. Particularly in fungi, analysis of differentially expressed and microbiome function prediction was performed by using subgroups where early-stage was divided in control, D1N, D2N, D2I; development-stage: D3E D3L, D4E and D4L; late-stage: D5E and D5L. Control corresponds to organisms

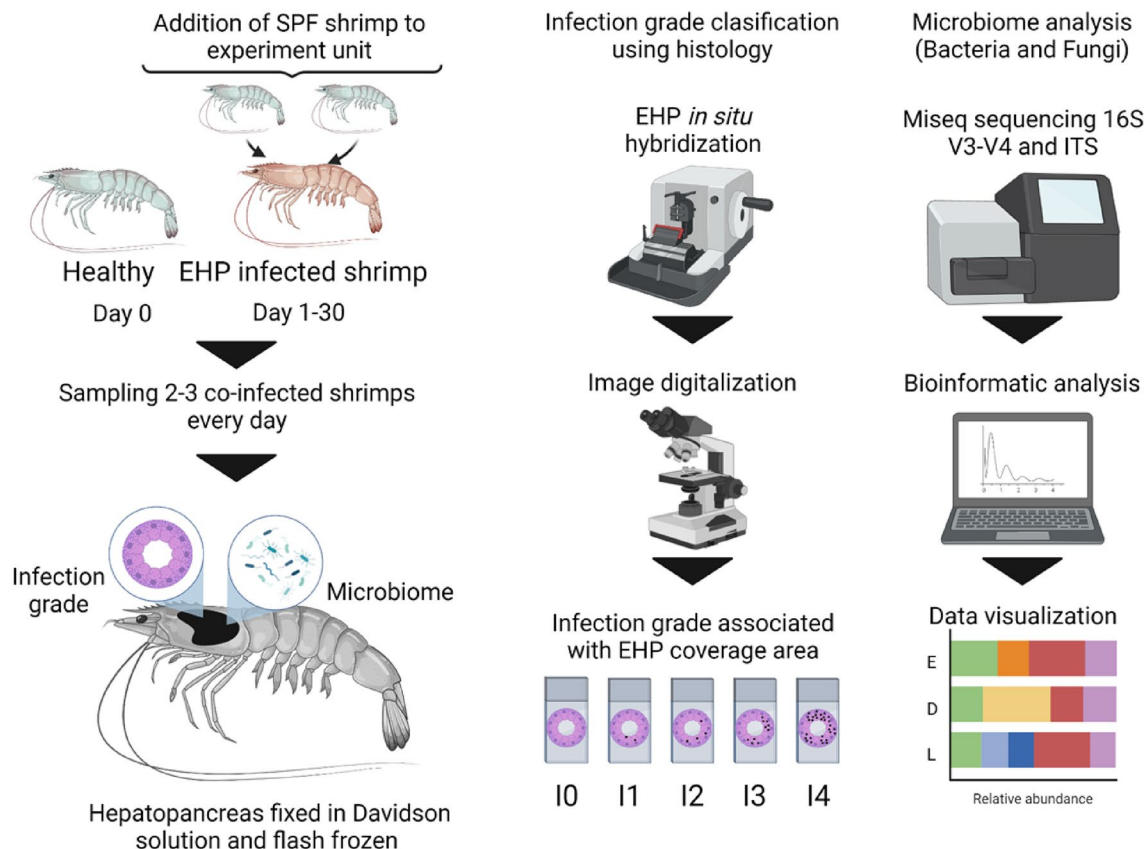


Figure 1. Work diagram and sampling collection. Experimental design to assess the bacterial and fungi community structure and predict hepatopancreatic microbiome functions in shrimp co-infected by EHP for 30 days. This image was created with BioRender (<http://biorender.com/>).

sampled on day 3; D1 on day 6; D2 on day 9 and 12; D3 on day 15 and 18; D4 on day 21 and 24; D5 on day 27 and 30. The N was used to describe non-infected organisms, I for infected organisms at the early disease stage, E for organisms with infection grades of I1 and I2, and L for organisms with infection grades of I3 and I4. These sub-groups were assessed in fungi taxa due to the variability pattern among samples.

Results

Digital histopathology: detection of EHP and quantification of the severity of infection. Five infections grades in the hepatopancreas of co-infected shrimp were assigned according to Lightner²¹: I0, I1, I2, I3 and I4 which were related ($P < 0.05$) to an EII value of 0%, 0.004–0.14%, 0.51–5.92%, 6.85–9.26% and 10.15–45.67% respectively (Fig. 2). A total of three stages of the disease were used to describe the infection cycle: early, development and late (Fig. 3A) which was supported by the EII assessed by infection grade (I0–I4) by each disease stage (early-late) (Fig. 3B) and mean value for each disease stage (Fig. 3C).

Due to the variability of the infection process of EHP, it was not possible to ensure replicates for each infection grade in each disease stage. For this reason, the statistics of microsporidiosis development were descriptive. The early-stage consisted of the first 12 post-infection days (dpi) where the lower EII mean value ($0.92 \pm 3.06\%$) was registered. EHP was only detected in one sampled shrimp on 9 and 12 dpi. After the early-stage, all sampled shrimp were positive to EHP (I1–I4). The development-stage started at 15 and ended at 24 dpi and was accompanied by the higher mean value of the EII ($8.08 \pm 13.75\%$). This stage was characterized by the abrupt increase of infected shrimp at high-infection grades (I3 and I4) and shrimp at I4 registered the highest EII values ($31.97 \pm 19.37\%$) throughout the bioassay. In the late-stage (at 27 to 30 dpi), the number of shrimp with a high infection intensity (I3 and I4) was reduced and the EII mean value decreased ($5.44 \pm 6.28\%$). At the late-stage, we observed what appears to be an asymptotic pattern where shrimp are in a cyclic infection process. According to these results, EHP proliferates possibly until shrimp reach infection grade I4 and then parasite load starts decreasing until shrimp reach infection grade I1. This pattern could be repeated throughout the culture cycle.

Microbiome composition analysis. For bacteria and fungi taxonomic assignments, a total of 532,841 and 658,492 non-chimeric sequence reads ($Q > 25$) were used for OTUs table construction using the Greengenes and UNITE database, respectively. A total of 1895 OTUs for bacteria and 213 OTUs for fungi were found and used as a reference for clustering libraries reads into OTUs. Among bacteria, the assigned taxonomic hierarchy classification allowed identifying two domains, bacteria (97–100%) and archaea (< 3%). A total of 20 bacteria (11 unclassified) and 3 archaea phyla were identified and classified further into 234 (215 unclassified) genera.

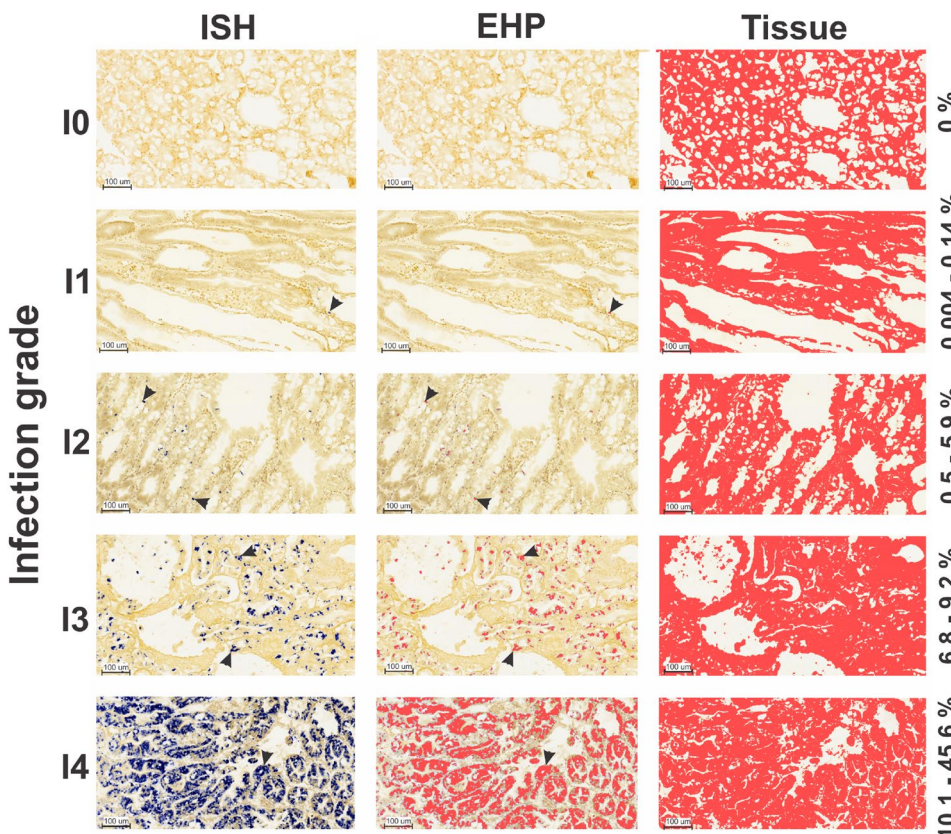


Figure 2. EHP infection intensity grade scale. Infection grade was assessed by in situ hybridization (ISH) using the EHP infection index (EII) and assigned by the methodology proposed by Lightner²¹. Each infection grade category (I0–I4) was represented for the first time by a value range of EII (%) shown at the right side of the image. The figure shows how the EHP and tissue area are separately quantified using $\times 10$ image to calculate the EII according to each infection stage proposed by Lightner²¹. Black arrows mark EHP detection.

Among fungi, one domain was identified, fungi. A total of 3 fungi phyla were identified and classified further into 32 (5 unclassified) genera.

The most representative phyla found among bacteria included Proteobacteria (12–98%), Firmicutes (1–24%) and Tenericutes (0.3–82%) (Fig. 4A) while Basidiomycota (0–99%) and Ascomycota (0–99%) were most abundant among fungi (Fig. 4B). Differences among disease stages at a phylum level were only seen in fungi domain, where a reduction of Ascomycota phyla was accompanied by an increase of the Basidiomycota phyla at the late-stage of the disease.

The most represented genera in bacteria were *Pseudomonas* (0.7–80%) (Fig. 4A) and in fungi *Naganishia* (0–97%) (Fig. 4B). In bacteria, *Pseudomonas*, *Comamonas*, *Agrobacterium*, *Delftia* and *Actinobacteria* were clustered separately from other genera such *Streptococcus*, *Anoxybacillus*, *Loktanella*, *Methylobacterium* and *Vibrio* (Fig. 4A). In fungi, most of the genera were clustered together except for *Naganishia* (Fig. 4B). This clustering allowed the identification of microorganisms that may be found in a particular microenvironment (e.g. physicochemical parameters and physiological stages of the host).

Microbiome modulation in shrimp hepatopancreas infected by EHP. According to the taxonomic differentially expressed analysis in bacteria ($P < 0.05$), a higher number of differentially expressed taxa were found in early-stage (59 taxa) compared to the development and late-stage (2 and 6 taxa, respectively). The genera *Pseudomonas*, *Comamonas* and *Agrobacterium* were highly related to the early-stage of the disease ($P < 0.05$), the class *Actinobacteria* to the development-stage ($P < 0.05$), and the genera *Leadbetterella*, *Aquimarina* and *Vibrio* to the late-stage of the disease ($P < 0.05$) (Fig. 5A). Differentially expressed bacteria ($P < 0.05$) at the different disease stages were phylogenetically different between disease stages (Fig. 5B). In the fungi domain, the genus *Komagataella* was related to the early-stage ($P < 0.05$), the genera *Naganishia* and *Alternaria* to the development-stage ($P < 0.05$) while the genus *Malassezia* was related to the late-stage ($P < 0.05$) (Fig. 5C). The fungi at different disease stages were not grouped by phylogenetic analysis (Fig. 5D). Some bacteria and fungi genera can be found in different disease-stages, but their abundance is associated to the disease stage.

Bacterial richness and diversity. Alpha diversity was assessed by Simpson index and Shannon index for diversity and Observed OTUs for richness. For bacteria, the diversity indexes in the shrimp hepatopancreas were

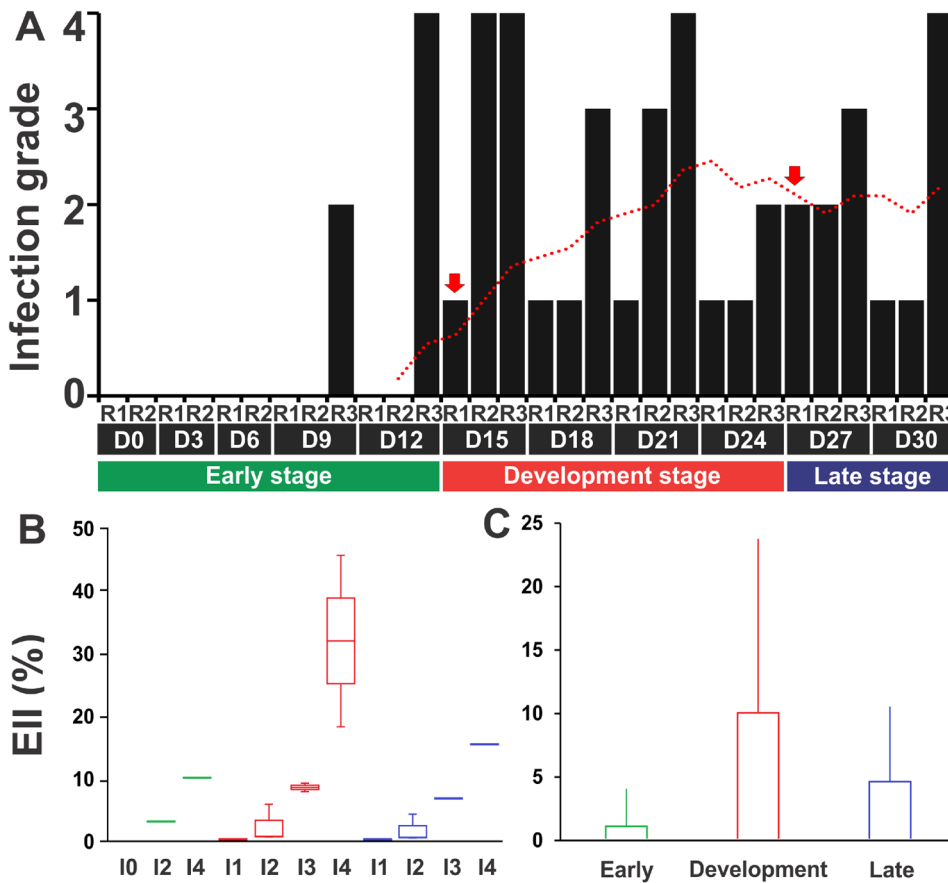


Figure 3. Evaluation of EHP infection. (A) EHP infection grade (I0–I4) registered during the bioassay and EHP infection index (EII) values according to (B) infection grade by each disease stage and (C) mean value for each disease stage. Black bars denote the infection grade of each organism sampled. The red dotted line represents the average of black bars considering 3 sampling days. Red arrows represent the beginning and the end of each disease stage. Color bars cluster the organisms from early (green), development (red), or late (blue) stages of the disease. R: replicate (sampled shrimp); D: day (sampling day). EII values are represented as mean \pm standard deviation.

high in all disease-stages (Fig. 6A), while in fungi the diversity indexes were low (Fig. 6B). Non-statistical differences were found between disease stage in bacteria and fungi using Simpson index ($P=0.15$, $P=0.77$), Shannon index ($P=0.12$, $P=0.71$) and Observed OTUs ($P=0.17$, $P=0.09$), respectively. However, in bacteria, a higher diversity was registered at the early-stage and a lower score at the late-stage. In contrast, in fungi, we observed an inverse pattern compared to bacteria.

In both bacteria and fungi, the beta diversity plotted in PCoA graphics separated organisms into two different groups ($P<0.05$). Shrimp in the early-stage of the disease were separated from shrimp at the development and late-stage. The same aggrupation was visualized in clustering replicate by Pearson's correlation (Fig. 6C,D). In some cases, organisms from the development-stage with the lowest infection grade were grouped with early-stage organisms. While some organisms from the early-stage with high infection grades (I2 and I4) were grouped with organisms at the development-stage (Fig. 6C,D).

Identification of microbiome functionality. The integration of LEfSe and PICRUSt results showed significant change ($P<0.05$) in the microbiome functionality among disease-stages. In general, we observed a transition from a healthy hepatopancreatic microbiome flora to a pathobiome. The microbiome function of bacteria at the early-stage of the disease ($P<0.05$) were mainly associated with membrane transporter, fatty acid biosynthesis and other metabolic pathways associated to nutrient acquisition (Fig. 7A). This was highly similar to the predicted microbiome functions of fungi at the early-stage (ABC transporters, lipid biosynthesis protein, among others) (Fig. 7B).

During the development-stage, although the microbiome of shrimp was still partially related to nutritional function, some pathways related to the bacteria transcription (e.g. ribosome and aminoacyl tRNA biosynthesis) processes in the bacteria group (Fig. 7A) and bacterial toxin production in the fungi group were registered ($P<0.05$) (Fig. 7B).

At the late-stage, most of the enriched metabolic pathways ($P<0.05$) in bacteria were different from those found in fungi. Bacterial microbiome predicted function ($P<0.05$) was mainly related to opportunistic or

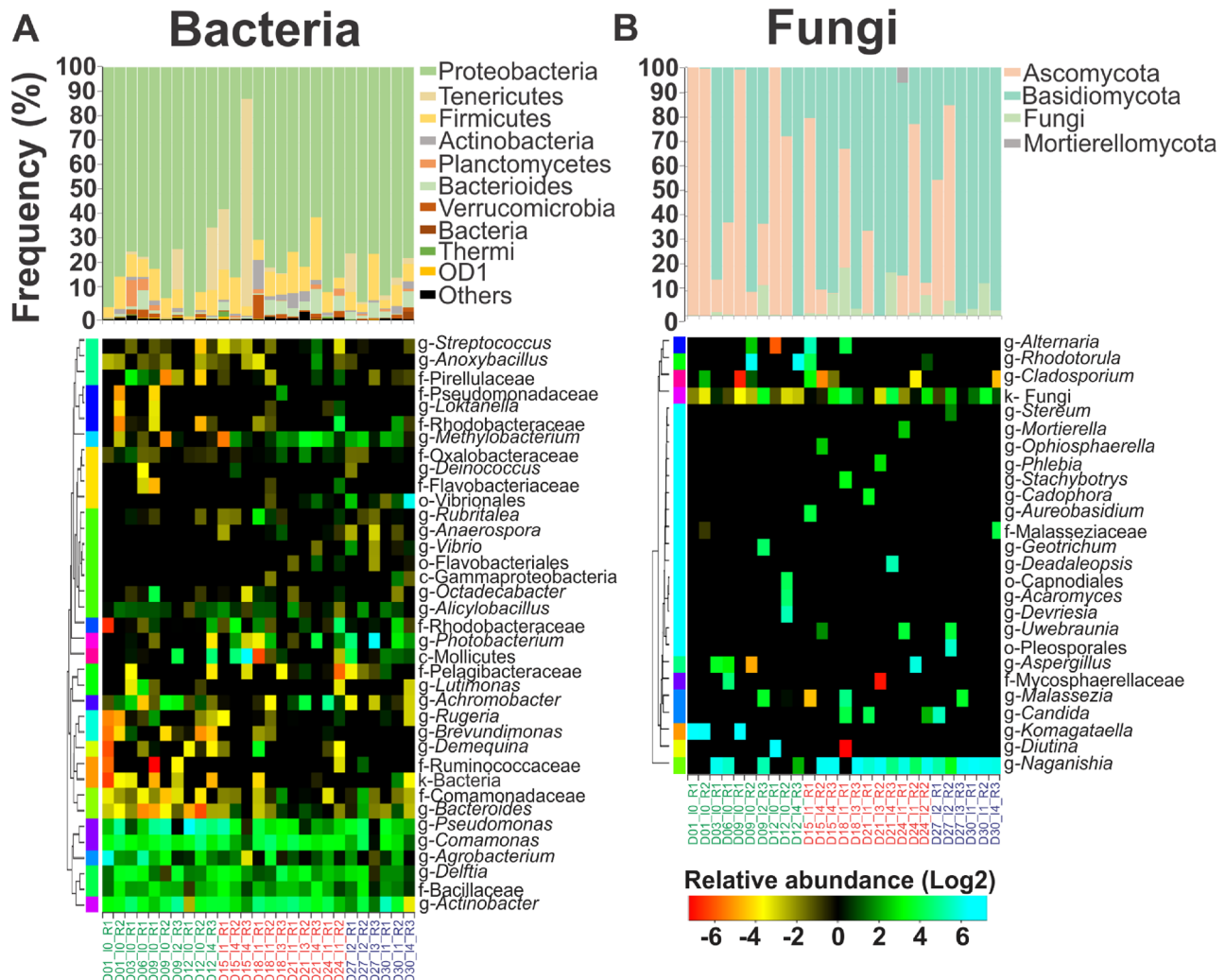


Figure 4. Shrimp microbiome at phyla and genera level registered at different disease stages. Microbiome modulation for (A) bacteria and (B) fungi taxa. Relative abundance is expressed as a percentage for phyla, where only phyla with higher relative abundance than 1% in at least one of the replicates are shown. Heatmaps using Log2 transformed relative abundance were used to cluster (y axis) genera present in similar conditions. Only genera with higher relative abundance than 1% in at least one of the replicates are shown. Shrimp were grouped (x axis) by the disease stage (early in green, development in red and late in blue) for easy visualization of the microbiome change between healthy and infected shrimp. The heatmaps color key ranges from orange for low abundant (< 1%) microorganisms to cyan for high abundant microorganisms (1–90%). Letters p- (phyla), c- (class), o- (order), f- (family) and g- (genera) on the left side of the taxa name represent the group level.

pathogenic bacteria proliferation and bacterial infection process (e.g. *Vibrio cholerae* pathogenic cycle and peptidoglycan biosynthesis) (Fig. 7A). The fungi microbiome predicted function were mainly related to protein and carbohydrates degradation (e.g. amino sugar and nucleotide sugar metabolism, peptidases and other glycan degradation) (Fig. 7B).

Discussion

Hepatopancreatic microsporidiosis (HPM) is an emergent threat to sustainable shrimp farming worldwide. Our understanding of host-pathogen interactions in HPM will allow the development of strategies to mitigate risk of disease outbreaks in shrimp farming. Our results show that infection by EHP in *P. vannamei* can be detected as early as 9 dpi when using the co-habitation challenge model coupled with in situ hybridization (ISH). The earlier detection of EHP in this study compared to other authors, that report EHP detection 14 dpi¹⁸, could be attributed to the differences in many exogenous (e.g. parasite load, water quality) and endogenous (e.g. physiological state) factor modulating the parasite's infection process in shrimp^{19,31}. In any case, the capability of detecting EHP in less than 10 dpi could have positive diagnostic implication since combining ISH and real-time PCR could be an effective means in detecting the parasite early in a culture cycle.

Our data revealed that EHP pathogenesis in challenged shrimp shows a well-defined pattern. During the first 12 dpi (early-stage), the presence of EHP was undetectable except for one organism at each day 9 and

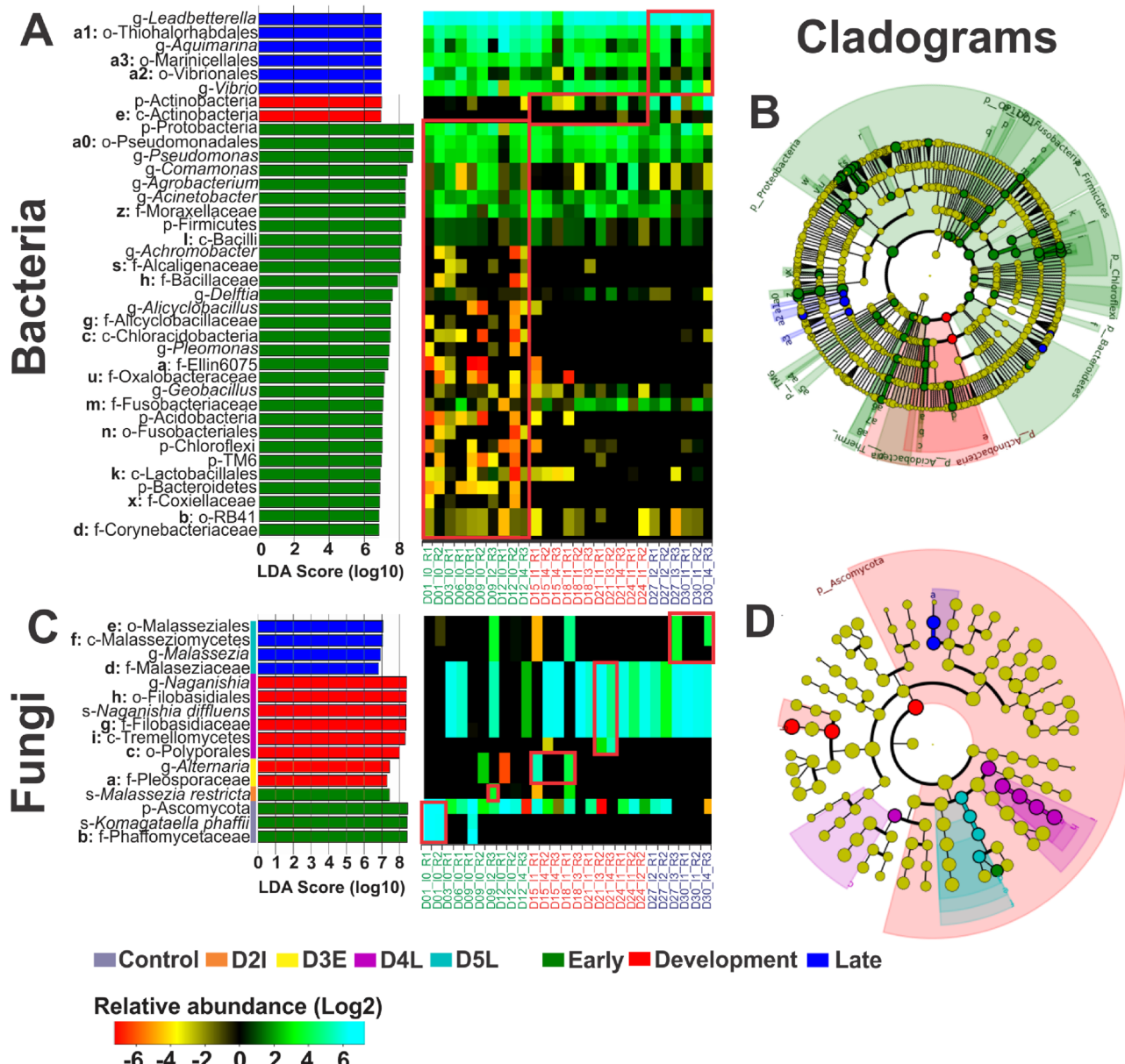


Figure 5. LEfSe results for enriched taxa of shrimp at early, development and late stage of the disease. Differentially expressed taxa visualized together with heatmap and cladogram graph for bacteria (A,B) and fungi (C,D), respectively. Differentially expressed taxa shown as log10 LDA score for each disease classification. Heatmaps using Log2 transformed relative abundance were used to cluster (x axis) genera by disease stage (early in green, development in red and late in blue). Red squares highlight the differentially expressed taxa in each disease stage condition. Cladograms represent the phylogenetic relation between microorganisms detected at the different disease stages and are marked with a bold alphabetical letter to locate the name of the taxa in the log10 LDA score graph. The heatmaps color key ranges from orange for low abundant (< 1%) microorganisms to cyan for high abundant microorganisms (1–90%). The top 30 overrepresented taxa are shown. Letters p- (phyla), c- (class), o- (order), f- (family) and g- (genera) on the left side of the taxa name represent the group level. For fungi, a subgroup of disease-stage was used: control and D2I from the early-stage, D3E and D4L for the development-stage and D5L for the late-stage. For fungi, subgroups of disease-stage were used: control, D1N, D2N, D2I for early-stage, D3E D3L, D4E and D4L for development-stage and D5E and D5L for late-stage.

12 dpi. This was followed by a development-stage where the pathogen proliferated in the hepatopancreatic tissue. Thereafter, shrimp entered the late-stage of disease progression which appears to have a cyclic infection pattern, where organisms from infection grade I4 might decrease to I1, and repeated the cycle, without reaching I0 again. To our knowledge, this is the first time that a cyclic pattern of EHP proliferation has been proposed in *P. vannamei*. Cyclic infection patterns have been previously related to chronic infections in mammals and in other invertebrates^{32,33}. The interaction between the host and the pathogen in chronic infections is long-lasting where the host is unable to deal with the pathogen over time and the pathogen feeds from the energetic reserve

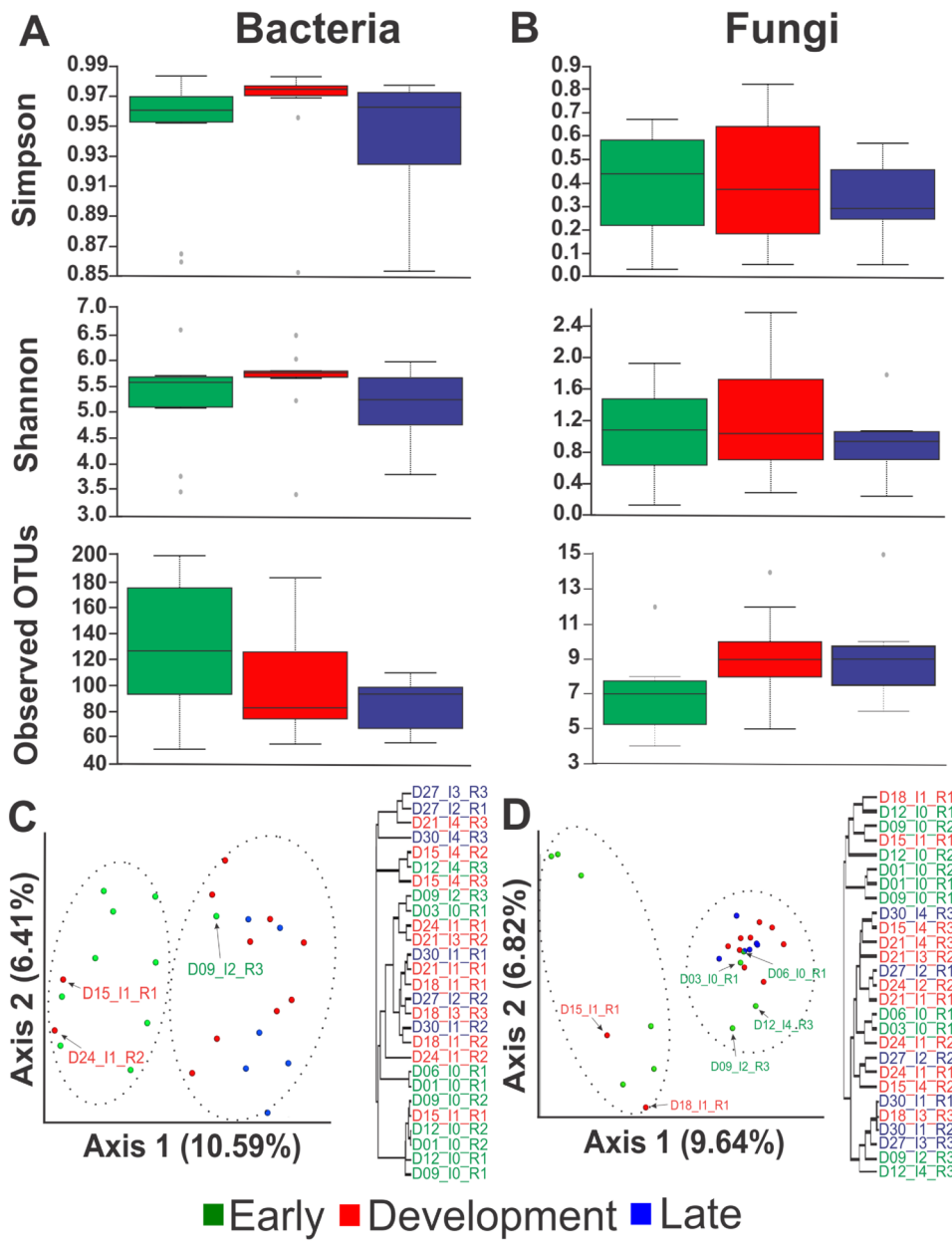


Figure 6. Box plots of three different alpha indexes and PCoA plot of beta index. Alpha indexes were assessed by Simpson and Shannon index and observed OTUs for (A) bacteria and (B) fungi. Beta index visualized with a PCoA and hierarchical clustering of Pearson's correlation for (C) bacteria and (D) fungi at different disease stages. The colors green (early), red (development) and blue (late) represent the groups of organisms at different disease stages.

from the host and/or use host cells to replicate^{3,34}. These interactions between parasite-host slowly deteriorate the host health causing slow growth and poor performance, as proposed for other microsporidians causing growth retardation in the bee *Apis cerana*³². Particularly, microsporidians have been reported to cause chronic persistent diseases that can vary in their infection intensity throughout the disease cycle^{32,33}, and in some cases, the pathogen cannot be detected in the infected organisms. However, infected organisms lacking clinical signs are able to transmit the infection³⁵. This information strongly supports our findings related to the disease pattern of EHP in *P. vannamei* where infection intensity can significantly decrease at late stage of the disease. It is interesting to point out, that this cyclic disease pattern may help explain why some studies fail to detect EHP in some shrimp displaying white feces syndrome³⁵. This syndrome has been associated to EHP under particular conditions and coinfections with certain strains of *Vibrio parahaemolyticus*³⁶.

Our data show that the cyclic pattern of EHP infection status is associated with a chronic infection that progressively deteriorates the microbiome community and its functionality, resulting in an outbreak of pathogenic and opportunistic bacteria and fungus. The phyla frequency of bacteria did not register a clear relation with the disease stage. However, in fungi, an increase of the Basidiomycota phyla accompanied by a decrease

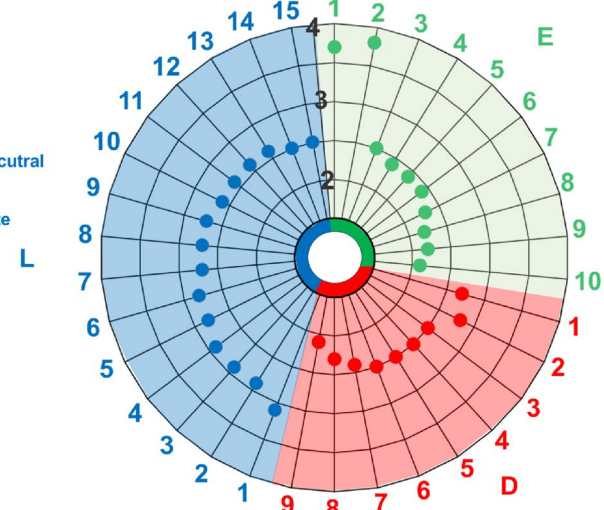
A Predicted microbiome function

1E.- Transporters	1L.- Otherion coupled transporter
2E.- ABC transporters	2L.- Ribosome biogenesis
3E.- Fatty acid biosynthesis	3L.- <i>Vibrio cholerae</i> pathogenic cycle
4E.- Tyrosine metabolism	4L.- Function unknown
5E.- Chlorocyclohexane and	5L.- Purine metabolism
Chlorobenzene degradation	6L.- Pyrimidine metabolism
6E.- Ascorbate and aldarate metabolism	7L.- Energy metabolism
7E.- Bisphenol degradation	8L.- Chaperone and folding catalysts
8E.- Isoflavonoid biosynthesis	9L.- Methan metabolism
9E.- Non Homologus and joining	10L.- Membrane and intracellular structural
10E.- Toluene degradation	molecules
1D.- Glyoxylate and dicarboxylate	11L.- Transition proteins
metabolism	12L.- Alanine, aspartate and glutamate
2D.- Ribosome	metabolism
3D.- Aminoacyl tRNA biosynthesis	13L.- Glycolysis - Glucogenesis
4D.- Pyruvate metabolism	14L.- Peptidoglycan biosynthesis
5D.- Valine leucine and isoleucine	15L.- Homologous recombination
biosynthesis	
6D.- Citrate cycle TCA cycle	
7D.- Pantothenate and CoA biosynthesis	
8D.- Caffeine metabolism	
9D.- Prenyltransferases	

B

1E.- ABC transporters	14D.- Synthesis and degradation of ketone bodies
2E.- Porphyrin and chlorophyll metabolism	15D.- Peroxisome
3E.- Lipid biosynthesis protein	16D.- Cytoskeleton proteins
4E.- Nicotinate and nicotinamide	17D.- Bacterial toxin
metabolism	18D.- Renin angiotensin system
5E.- Tropane piperidine and pyridine	19D.- Glycosaminoglycan degradation
alkaloid biosynthesis	20D.- Nucleotide metabolism
6E.- Isoquinoline alkaloid biosynthesis	
7E.- Protein processing endoplasmic	1D.- Amino sugar and nucleotide sugar
reticulum	metabolism
8E.- Glycosphingolipid biosynthesis	2D.- Peptidases
ganglio series	3D.- Fructose and manose metabolism
9E.- Biosynthesis of vancomycin group	4D.- Galactose metabolism
antibiotics	5D.- Strach and sucrose metabolism
10E.- Type I diabetes mellitus	6D.- Pentophosphate pathway
11E.- Cellular antigens	7D.- Other glycan degradation
12E.- RIG I like receptors signal pathway	8D.- Streptomycin degradation
1D.- Phosphotransferase system PTS	9D.- Sphingolipid metabolism
2D.- Other	10D.- Lysosome
3D.- Valine leucine and isoleucine	11D.- Polyketide sugar unit biosynthesis
degradation	12D.- Glycosphingolipid biosynthesis globo
4D.- Fatty acid metabolism	series
5D.- Propanoate metabolism	13D.- Butirosin and neomycin biosynthesis
6D.- Butanoate metabolism	14D.- Secondary bile acid biosynthesis
7D.- Tryptophan metabolism	
8D.- Lysine degradation	
9D.- Beta alanine metabolism	
10D.- Geraniol degradation	
11D.- Limonene and pinene degradation	
12D.- Caprolactam degradation	
13D.- Nucleotid excision repair	

Bacteria



Fungi

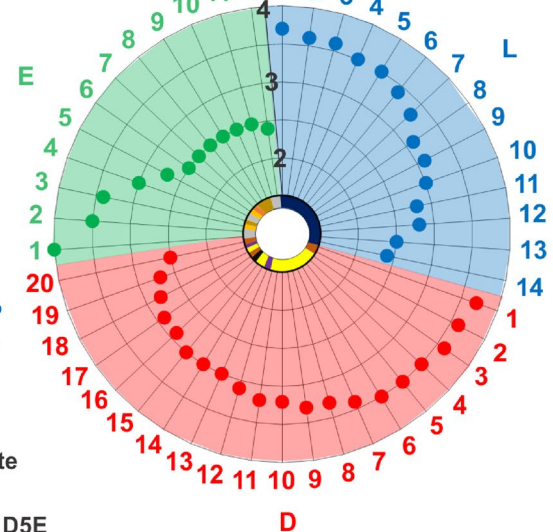


Figure 7. Difference of enriched KEGG metabolic pathways between disease stages groups. The graph shows the predicted microbiome functions according to (A) bacteria and (B) fungi found at the early (E; green), development (D; red) and late (L; blue) stages of the disease. Circular graphs show log10 LDA score (1–4) of the enriched KEGG metabolic pathways. For fungi, subgroups of disease-stage were used: control, D1N, D2N, D2I for early-stage, D3E, D3L, D4E and D4L for development-stage and D5E and D5L for late-stage. This image was created using EasyMAP¹⁷ and KEGG database⁶⁴.

of the Ascomycota phyla was registered at the end of the development-stage and the late-stage of the disease. The Ascomycota phylum was registered at the early-stage of the disease, which was expected as it is the most abundant phyla in a healthy shrimp hepatopancreas²⁸. The increase of the Basidiomycota phyla at the late-stage was associated with an increase of the genus *Malasseiza*, which has been associated as a pathogen of marine organisms³⁷. This suggests that pathogenic fungi from Basidiomycota phyla proliferate in EHP-infected shrimp gradually replacing beneficial fungi from the Ascomycota phyla. It was interesting to note that the Microsporidian phylum was not registered in our curated fungal sequences originating from EHP-infected shrimp. This was attributed to the absence of EHP ITS amplification. Although, ITS is proposed as a universal DNA barcode biomarker for fungi³⁸, microsporidian rDNA units are dispersed throughout the genome in some species, resulting in the non-amplification of the ITS region³⁹.

At a bacterial genus level, a higher abundance of *Bacteroides*, *Pseudomonas*, *Acinetobacter*, *Delftia*, *Agrobacterium*, *Achromobacter* and *Comamonas* was recorded at the early-stage and clustered within them. The clustering

between these bacteria indicates that they may be related to a similar environmental condition in a particular habitat (hepatopancreas) and to a healthy status of the host as all these taxa have been registered in healthy *P. vannamei* shrimp^{11,40–42}. The beneficial activity of these taxa is highly related to their previously reported functions in the host digestive system. The genera *Bacteroides* and *Comamonas* spp. have been reported to be major producers of vitamin B12⁴³ along with antimicrobial metabolites in *Comamonas* spp.^{44,45}. The *Pseudomonas* genus has been related to increase in digestive enzymes activity¹¹ and pathogen resistance⁴⁰ in *P. vannamei*. The genera *Achromobacter* and *Acinetobacter* have been reported in shrimp gut and include nitrifying and denitrifying bacteria, which may be related to the improvement of water quality^{46,47}. Bacteria from the genus *Agrobacterium* have been related to increased lipid absorption in alpine trout (*Salvelinus alpinus*)⁴⁸. Finally, the genera *Delftia* have been used to reduce the virulence of gram-negative pathogens⁴⁹. Additionally, the loss of members of the families Comamonadaceae and Bacteroides genera have been previously reported in *P. vannamei* infected with EHP⁴². The above supports the hypothesis that those bacterial taxa from the early-stage of the disease are essential for health and improvement of the digestive system homeostasis in *P. vannamei*. This also suggests that EHP modified the hepatopancreas environment which results in the displacement of these beneficial bacteria.

It is worth noting even though *Acinetobacter* and *Delftia* genera were registered in the early-stage and have been associated with healthy shrimp, other authors have reported that those genera can be pathogenic for shrimp^{50,51}. This indicates a healthy microbiome balance not only depends on the absence or presence of certain taxa but also on their abundance¹². Among fungi, only the genus *Komagataella* was associated with the early-stage of the disease related to the species *K. phaffii*. However, to our knowledge, it has not been reported in *P. vannamei* shrimp and is the first time that is being related to a good health status in *P. vannamei*.

Contrary to the early-stage, during the developmental stage, a lower number of bacterial taxa was differentially expressed compared to fungi suggesting a higher proliferation of fungi species at this stage. Low overrepresentation of bacteria taxa may be a consequence of antagonistic interactions among beneficial, commensal and pathogenic microorganisms as the disease begins to progress. Only one bacterial taxon was overrepresented at the development-stage of the disease and corresponded to class Actinobacteria. This class has been detected in healthy shrimp¹¹, related to antifungal properties⁵², antagonistic activity against pathogenic *Vibrio* spp.⁵³ and related to shrimp infected with EHP⁴². This suggests a higher modulation of the Actinobacteria class due to EHP proliferation during the development-stage of the disease. Considering the antifungal properties of this class⁵², its overrepresentation could be explained as it is harder to displace these bacteria by EHP or other opportunistic and pathogenic fungus genera such *Naganishia* and *Alternaria* which were the most overrepresented fungi taxa at the development-stage. The effect of *Naganishia* and *Alternaria* genera on the health of *P. vannamei* shrimp has not been clearly assessed yet. However, these fungi are considered opportunistic pathogens in humans^{28,54}. This indicates that during the development-stage of the disease the shrimp's digestive systems start to lose the community structure and balance of the microbiome. The development stage could be described as a transition zone, where beneficial bacteria is being displaced and opportunistic fungi begins to proliferate.

At the late-stage of the disease, a displacement of beneficial bacteria was very evident and proliferation of the pathogenic bacteria genera like *Vibrio* and *Aquimarina* and pathogenic fungus genera like *Malassezia* were registered. These bacterial and fungal genera have been considered opportunistic pathogens^{37,55,56} supporting the hypothesis that EHP at the late-stage of the disease generates a dysbiosis process in the hepatopancreas of *P. vannamei* that enables proliferation of opportunistic microorganisms. An increase of vibrio abundance have been related to dysbiosis¹⁰, and EHP infection in *P. vannamei*²⁷. The genera *Aquimarina* has been also related to disease in crustaceans causing mortalities in *P. vannamei* larvae⁵⁷ and increased abundance of *Malassezia* sp. has been reported in white feces disease in *P. vannamei*⁵⁸ that can be caused due to coinfection with EHP and *V. parahaemolyticus*³⁶. Further investigation will unravel role of *Aquimarina* and *Malassezia* in shrimp health and understanding if these bacteria are commensals that turn pathogenic once the EHP contributes to specific host environmental changes. Interestingly the bacteria genera *Leadbetterella* was also overrepresented at the late-stage. However, due to this genera being linked to healthy shrimp treated with probiotics⁵⁹, its role in shrimp needs to be further investigated.

Based on our data, as exposure time with EHP progresses, beneficial microorganisms showed reduce abundance or are displaced and commensal, opportunistic and pathogen start to proliferate. Also, some microorganisms cannot be considered as beneficial or pathogenic as their role will depend on the physico-chemical properties of the digestive system⁶⁰ and the interactions with the community of the microbiome⁶⁰ which are being altered by EHP. It is important to note that while some microbiome changes could be related to SPF shrimp adjusting to new environmental conditions (tank in which the animals were reared) the microbiome community/functions that were observed strongly support that EHP is the main driver of hepatopancreas microbiome/microenvironment changes. Particularly, the proliferation of opportunistic/pathogenic microorganisms was more evident at the late stage in organisms with higher infection grades compared with those with lower infection grades. Furthermore, as mentioned above, the existing literature on microbiota alteration and the presence of certain microorganisms related to EHP infection in penaeids align with our observations.

The differences in microorganism abundances (higher differentially expressed taxa at the early-stage) registered between disease stages, were according to the results obtained from the diversity index in bacteria. Although no significant differences were found in the bacterial alpha index among disease stages, the beta index significantly separated the early-stage from the development and late-stage of the disease indicating a shift in

the microbiome community and diversity¹². As expected, the lower diversity bacteria values were registered at the late-stage of the disease. Similar findings have been previously reported where lower alpha diversity values are registered in diseased organisms, but no significant differences were detected⁴². This supports the fact that diseased condition reduces bacterial alpha diversity in *P. vannamei* digestive system which is accompanied by dysbiosis^{10,12,61}. The reduction in microorganisms' diversity is attributed to opportunistic pathogens that out-compete commensal and beneficial bacteria, and cause and outbreak in the shrimp digestive system^{12,61}. It must be highlighted that in our study the microbiome diversity of SPF shrimp before the infection was the lowest recorded in all the experimental trials, which may increase variability in the experimental design when assessing microorganisms' diversity. This low microbial diversity of the SPF shrimp was attributed to the fact that laboratory maintained animals are not exposed to a high diversity of microorganisms, unlike farmed shrimp¹³.

Contrary to bacteria, the alpha diversity in fungi increased at the late-stage of the disease. The reduction of diversity in fungi has been reported in diseased shrimp²⁸. In our study, the increase in diversity was associated with a proliferation of opportunistic pathogenic fungi at the late-stage which was related to member of the Basidomycota phylum. The abundance of the members belonging to this phylum has been considered as an indicator of dysbiosis in shrimp⁶¹. The inverse pattern in fungal diversity compared to bacteria may be associated with a possible improvement of the hepatopancreas environment caused by EHP for opportunistic pathogenic fungi. It is known that microsporidian damages the hepatopancreas cells³ this may increase dead hepatopancreatic epithelial cells that sloughed off into the lumen of hepatopancreatic tubule. We speculate that the detachment of epithelial cells from the basal membrane exposes the underlying tissue and thus creating a right niche for the proliferation of the Basidomycota phyla.

The predicted functionality of the microbiome was closely related to the overrepresented taxa at each stage of EHP infection cycle. As mentioned earlier, the bacteria and fungi taxa at the early-stage of the disease were highly associated with nutrient acquisition which was supported by the enriched metabolic pathway results. At the early-stage of the disease, the overrepresented pathways in bacteria and fungi were ABC transporters and fatty acid biosynthesis which are highly associated with digestion and absorption of nutrients but also to higher performance of the defense systems^{41,62}. Some of these microbiome functions have been reported in healthy shrimp⁴⁰ supporting the importance of microorganisms in nutrient acquisition and the health of the host⁴¹.

At the development-stage, which could be considered as a transition zone, a healthy microbiome starts to lose balance due to an increase in interactions between beneficial and opportunistic pathogenic microorganisms. However, at the late-stage of the disease, a loss of metabolic pathways related to nutrient acquisition was registered for members of both bacteria and fungi domains. This was previously postulated by Duan et al.⁴² who mention that EHP may influence nutrient absorption by intestine bacteria that corroborates the effect of EHP infection over the nutrient intake by shrimp. Interestingly, at the late-stage of the disease, the enriched metabolic pathways from bacteria and fungi were completely different. In bacteria, metabolic pathways were related to pathogenic bacteria proliferation (*Vibrio cholerae* pathogenic cycle, peptidoglycan biosynthesis, homologous recombination). The reported immunosuppression in *P. vannamei* infected by EHP, which is accompanied by a dysbiosis process²⁷, could explain the proliferation of pathogenic bacteria (*Vibrio* and *Aquimarina* genera) that were registered in this study.

In fungi, most of the enriched metabolic pathways were associated with carbohydrates metabolisms including glycan degradation. This suggests that fungus at the late-stage may take advantage of the carbohydrate reserves of EHP-infected shrimp. This hypothesis is supported by transcriptomic, proteomic and metabolomic analyses where energy metabolism pathway such as carbohydrates degradation, digestion and absorption are regulated by EHP infection^{42,63}. Based on our findings, we propose EHP infection results in a cyclic chronic degenerative process that causes dysbiosis (Fig. 8). We speculate that EHP proliferates when the hepatopancreas reserves are high achieving a high infection intensity (I4) and as nutrient reserves are depleted pathogen proliferation halts or decreases. If conditions are favorable shrimp will temporarily recover and the hepatopancreas will once again become favorable niche for EHP.

Conclusions

Hepatopancreatic microsporidiosis caused by EHP in *P. vannamei* can be cataloged as a cyclic chronic degenerative infection where the healthy microbiome begins to lose diversity, beneficial microorganisms, and functionality related to nutrient acquisition and host health (dysbiosis). The longer EHP infection continues at a higher infection intensity a more evident alteration of the hepatopancreas microbiome will be observed. We determined EHP infection favors the increase in the abundance of bacterial from genera *Vibrio*, *Aquimarina* and *Leadbetterella* and in the fungal genus, *Malassezia*. Candidate beneficial microorganisms that are displaced during EHP infection include beneficial bacteria such as *Bacteroides*, *Pseudomonas*, *Acinetobacter*, *Delftia*, *Agrobacterium*, *Achromobacter*, *Comamonas* as well as species belonging to the family *Bacillaceae*, and the fungal genus *Komagataella*. Some members of these taxon's could be cultured and employed as probiotics to alleviate HPM disease progression. In addition, this is the first time, a quantitative histological approach was used to study the EHP infection cycle in the context of the microbiome changes in the shrimp hepatopancreas.

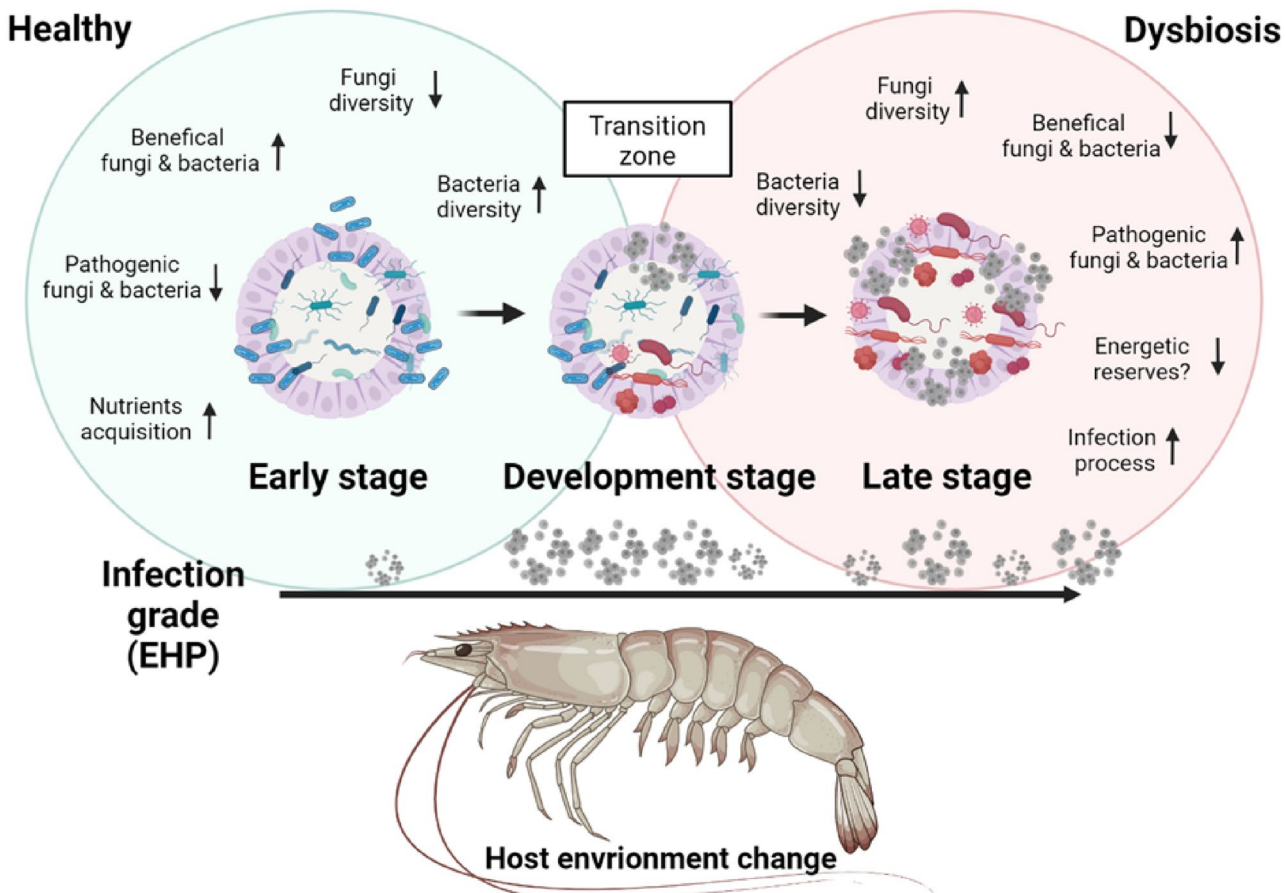


Figure 8. Modulation of the microbiome in the hepatopancreas of shrimp (*P. vannamei*) infected with EHP. Schematic diagram that represents the main changes produced in the host hepatopancreatic environment during the infection of EHP (30 days) according to the disease stages registered in this study. Infection intensity represents the cyclic pattern of EHP, where bigger EHP figures represent higher infection grade and smallest EHP figures represent lower infection grade. Blue bacteria: beneficial microbiota; Gray dots: EHP; Red bacteria: opportunistic and pathogenic microbiota. This image was created with BioRender (<http://biorender.com/>).

Data availability

16S rRNA V3-V4 and ITS amplicon sequencing datasets that support the conclusions of this article were deposited in NCBI under accession number PRJNA823752. All other relevant data are included as supporting information files and within the manuscript.

Received: 2 April 2022; Accepted: 24 August 2022

Published online: 30 August 2022

References

- FAO. *The State of World Fisheries and Aquaculture 2020: Sustainability in Action* (Food & Agriculture Organization, 2020).
- Chayaburakul, K., Nash, G., Pratanpipat, P., Sriurairatana, S. & Withyachumnarnkul, B. Multiple pathogens found in growth-retarded black tiger shrimp *Penaeus monodon* cultivated in Thailand. *Dis. Aquat. Organ.* **60**, 89–96. <https://doi.org/10.3354/dao060089> (2004).
- Tourtip, S. *et al.* *Enterocytozoon hepatopenaei* sp. nov. (Microsporidia: Enterocytozoonidae), a parasite of the black tiger shrimp *Penaeus monodon* (Decapoda: Penaeidae): Fine structure and phylogenetic relationships. *J. Invertebr. Pathol.* **102**, 21–29. <https://doi.org/10.1016/j.jip.2009.06.004> (2009).
- Thitamadee, S. *et al.* Review of current disease threats for cultivated penaeid shrimp in Asia. *Aquaculture* **452**, 69–87. <https://doi.org/10.1016/j.aqua.2015.10.028> (2016).
- Kooloth Valappil, R., Stentiford, G. D. & Bass, D. The rise of the syndrome—Sub-optimal growth disorder in farmed shrimp. *Rev. Aquac.* **13**, 1–19. <https://doi.org/10.1111/raq.12550> (2021).
- Munkongwongsiri, N. *et al.* *Enterocytozoon hepatopenaei* (EHP) spores are inactivated in 1 min at 75 °C. *Aquaculture* **533**, 736178. <https://doi.org/10.1016/j.aqua.2020.736178> (2021).
- Patil, P. K. *et al.* Economic loss due to diseases in India shrimp farming with special reference to *Enterocytozoon hepatopenaei* (EHP) and white spot syndrome virus (WSSV). *Aquaculture* **533**, 736231. <https://doi.org/10.1016/j.aqua.2020.736231> (2021).
- Karunasagar, I. & Ababouch, L. Shrimp viral diseases, import risk assessment and international trade. *Indian J. Virol.* **23**, 141–148. <https://doi.org/10.1007/s13337-012-0081-4> (2012).
- Flegel, T. W. A future vision for disease control in shrimp aquaculture. *J. World Aquac. Soc.* **50**, 249–266. <https://doi.org/10.1111/jwas.12589> (2019).

10. Holt, C. C., Bass, D., Stentiford, G. D. & Giezen, M. Understanding the role of the shrimp gut microbiome in health and disease. *J. Invertebr. Pathol.* **186**, 107387. <https://doi.org/10.1016/j.jip.2020.107387> (2021).
11. Rajeev, R., Adithya, K. K., Kiran, G. S. & Selvin, J. Healthy microbiome: A key to successful and sustainable shrimp aquaculture. *Rev. Aquac.* **13**, 238–258. <https://doi.org/10.1111/raq.12471> (2021).
12. Infante-Villamil, S., Huerlimann, R. & Jerry, D. R. Microbiome diversity and dysbiosis in aquaculture. *Rev. Aquac.* **13**, 1077–1096. <https://doi.org/10.1111/raq.12513> (2021).
13. Alberdi, A., Andersen, S. B., Limborg, M. T., Dunn, R. R. & Gilbert, M. T. P. Disentangling host–microbiota complexity through hologenomics. *Nat. Rev. Genet.* <https://doi.org/10.1038/s41576-021-00421-0> (2021).
14. Amenyogbe, E. *et al.* The exploitation of probiotics, prebiotics and synbiotics in aquaculture: present study, limitations and future directions: A review. *Aquac. Int.* **28**, 1017–1041. <https://doi.org/10.1007/s10499-020-00509-0> (2020).
15. Romano, N. Probiotics, prebiotics, biofloc systems, and other biocontrol regimens in fish and shellfish aquaculture. In *Aquaculture Pharmacology* (eds. Kibenge, F. S. B., Baldissarotto, B. & Chong, R. S. M.) 219–242 (Academic Press, 2021).
16. Dawood, A., Zuberi, A. & Shi, W. Plant-based β -mannanase supplemented diet modulates the gut microbiota and up-regulates the expression of immunity and digestion-related genes in *Cyprinus carpio*. *J. Appl. Anim. Res.* **50**, 21–30. <https://doi.org/10.1080/09712119.2021.2018327> (2022).
17. Hung, Y. M., Lu, T. P., Tsai, M. H., Lai, L. C. & Chuang, E. Y. EasyMAP: A user-friendly online platform for analyzing 16S ribosomal DNA sequencing data. *New Biotechnol.* **63**, 37–44. <https://doi.org/10.1016/j.nbt.2021.03.001> (2021).
18. Salachan, P. V., Jaroenlak, P., Thitamadee, S., Itsathitphaisarn, O. & Sritunyalucksana, K. Laboratory cohabitation challenge model for shrimp hepatopancreatic microsporidiosis (HPM) caused by *Enterocytozoon hepatopenaei* (EHP). *BMC Vet. Res.* **13**, 9. <https://doi.org/10.1186/s12917-016-0923-1> (2017).
19. Mai, H. N., Cruz-Flores, R., Aranguren Caro, L. F., White, B. N. & Dhar, A. K. A. Comparative study of *Enterocytozoon hepatopenaei* (EHP) challenge methods in *Penaeus vannamei*. *J. Invertebr. Pathol.* **171**, 107336. <https://doi.org/10.1016/j.jip.2020.107336> (2020).
20. Cruz-Flores, R., Mai, H. N., Noble, B. L., Schofield, P. J. & Dhar, A. K. Detection of *Enterocytozoon hepatopenaei* using an invasive but non-lethal sampling method in shrimp (*Penaeus vannamei*). *J. Microbiol. Methods* **162**, 38–41. <https://doi.org/10.1016/j.mimet.2019.05.008> (2019).
21. Lightner, D. V. *A Handbook of Shrimp Pathology and Diagnostic Procedures for Diseases of Cultured Penaeid Shrimp* (ed. Lightner, D. V.) 306 (World Aquaculture Society, 1996).
22. López-Carvalho, J. A. *et al.* Carbohydrate-rich diets meet energy demands of gametogenesis in hatchery-conditioned mussels (*Modiolus capax*) at increasing temperatures. *J. Shellfish Res.* **36**, 649–657. <https://doi.org/10.2983/035.036.0314> (2017).
23. Caporaso, J. *et al.* QIIME allows analysis of high-throughput community sequencing data. *Nat. Methods* **7**, 335–336. <https://doi.org/10.1038/nmeth.f.303> (2010).
24. Segata, N. *et al.* Metagenomic biomarker discovery and explanation. *Genome Biol.* **12**, R60. <https://doi.org/10.1186/gb-2011-12-6-r60> (2011).
25. Langille, M. *et al.* Predictive functional profiling of microbial communities using 16S rRNA marker gene sequences. *Nat. Biotechnol.* **31**, 814–821. <https://doi.org/10.1038/nbt.2676> (2013).
26. Andrews, S. *FastQC: A Quality Control Tool for High Throughput Sequence Data*. (Babraham Institute, 2019). <http://www.bioinformatics.babraham.ac.uk/projects/fastqc>.
27. Shen, H. *et al.* The links among *Enterocytozoon hepatopenaei* infection, growth retardation and intestinal microbiota in different sized shrimp *Penaeus vannamei*. *Aquat. Rep.* **21**, 100888. <https://doi.org/10.1016/j.aqrep.2021.100888> (2021).
28. Li, J., Jiang, H., Li, L., Zhang, X. & Chen, J. The Effect of disease and season to hepatopancreas and intestinal mycobiota of *Litopenaeus vannamei*. *Front. Microbiol.* **10**, 889. <https://doi.org/10.3389/fmicb.2019.00889> (2019).
29. Xue, M. *et al.* White spot syndrome virus (WSSV) infection alters gut histopathology and microbiota composition in crayfish (*Procambarus clarkii*). *Aquat. Rep.* **22**, 101006. <https://doi.org/10.1016/j.aqrep.2022.101006> (2022).
30. Warnes, G. R. *et al.* gplots: Various R Programming Tools for Plotting Data. <http://cran.r-project.org/web/packages/gplots/index.html> (2022).
31. Nkuba, A. C., Mahasri, G., Lastuti, N. D. R. & Mwendolwa, A. A. Correlation of nitrite and ammonia concentration with prevalence of *Enterocytozoon hepatopenaei* (EHP) in shrimp (*Litopenaeus vannamei*) on several super-intensive ponds in East Java, Indonesia. *JIPK* **13**, 58–67. <https://doi.org/10.20473/jipk.v13i1.24430> (2021).
32. Long, Q. *et al.* Impact of *Nosema ceranae* invasion on sucrose solution, midgut epithelial cell structure, and lifespan of *Apis cerana cerana* workers. <https://doi.org/10.1101/2022.01.09.475580v1> (2022).
33. Weiss, L. M. & Reinke, A. *Microsporidia Current Advances in Biology* (eds. Weiss, L. M. & Reinke, A.) 415 (Springer Nature Switzerland, 2022).
34. Bajgar, A. & Dolezal, T. Extracellular adenosine modulates host-pathogen interaction through regulation of systemic metabolism during immune response in *Drosophila*. *PLoS Pathog.* **14**, e1007022. <https://doi.org/10.1371/journal.ppat.1007022> (2018).
35. Tangprasittipap, A. *et al.* The microsporidian *Enterocytozoon hepatopenaei* is not the cause of white feces syndrome in whiteleg shrimp *Penaeus (Litopenaeus) vannamei*. *BMC Vet. Res.* **9**, 139. <https://doi.org/10.1186/1746-6148-9-139> (2013).
36. Aranguren-Caro, L. F. *et al.* Experimental reproduction of White Feces Syndrome in whiteleg shrimp, *Penaeus vannamei*. *PLoS One.* **16**, e0261289. <https://doi.org/10.1371/journal.pone.0261289> (2021).
37. Pang, K. L. *et al.* Pathogenic fungi of marine animals: A taxonomic perspective. *Fungal Biol. Rev.* **38**, 92–106. <https://doi.org/10.1016/j.fbr.2021.03.008> (2021).
38. Schöch, C. L. *et al.* Nuclear ribosomal internal transcribed spacer (ITS) region as a universal DNA barcode marker for Fungi. *Proc. Natl. Acad. Sci. USA* **109**, 6241–6246. <https://doi.org/10.1073/pnas.1117018109> (2012).
39. Ironside, J. E. Diversity and recombination of dispersed ribosomal DNA and protein coding genes in microsporidian. *PLoS One.* **8**, e55878. <https://doi.org/10.1371/journal.pone.0055878> (2013).
40. Cornejo-Granados, F. *et al.* Microbiome of Pacific Whiteleg shrimp reveals differential bacteria community composition between Wild, Aquaculture and AHPND/EMS outbreak conditions. *Sci. Rep.* **7**, 11783. <https://doi.org/10.1038/s41598-017-11805-w> (2017).
41. Li, E. *et al.* Gut microbiota and its modulation for healthy farming of pacific white shrimp *Litopenaeus vannamei*. *Rev. Fish. Sci. Aquac.* **26**, 381–399. <https://doi.org/10.1080/23308249.2018.14405302018> (2018).
42. Duan, Y. *et al.* Response signatures of *Litopenaeus vannamei* to natural *Enterocytozoon hepatopenaei* infection revealed by the integration of the microbiome and transcriptome. *Aquaculture* **542**, 736885. <https://doi.org/10.1016/j.aquaculture.2021.736885> (2021).
43. Tsuchiya, C., Sakata, T. & Sugita, H. Novel ecological niche of *Cetobacterium somerae*, an anaerobic bacterium in the intestinal tracts of freshwater fish. *Lett. Appl. Microbiol.* **46**, 43–48. <https://doi.org/10.1111/j.1472-765X.2007.02258.x> (2008).
44. Skariyachan, S. *et al.* Secondary metabolites extracted from marine sponge associated *Comamonas testosterone* and *Citrobacter freundii* as potential antimicrobials against MDR pathogens and hypothetical leads for VP40 matrix protein of Ebola virus: an in vitro and in silico investigation. *J. Biomol. Struct. Dyn.* **34**, 1865–1883. <https://doi.org/10.1080/07391102.2015.1094412> (2016).
45. Akduman, N. *et al.* Bacterial vitamin B12 production enhances nematode predatory behavior. *ISME J.* **14**, 1494–1507. <https://doi.org/10.1038/s41396-020-0626-2> (2020).
46. Kathiravan, V. & Krishnani, K. K. *Pseudomonas aeruginosa* and *Achromobacter* sp.: Nitrifying aerobic denitrifiers have a plasmid encoding for denitrifying functional genes. *World J. Microbiol. Biotechnol.* **30**, 1187–1198. <https://doi.org/10.1007/s11274-013-1543-6> (2014).

47. Shao, Y., Zhong, H., Mao, X. & Zhang, H. Biochar-immobilized *Sphingomonas* sp. and *Acinetobacter* sp. isolates to enhance nutrient removal: Potential in crab aquaculture. *Aquac. Environ. Interact.* **12**, 251–262. <https://doi.org/10.3354/aei00364> (2020).
48. Ringo, E., Strøm, E. & Tabacheck, J. Intestinal microflora of salmonids: A review. *Aquac. Res.* **26**, 773–789. <https://doi.org/10.1111/j.1365-2109.1995.tb00870.x> (1995).
49. Christiaen, S. E. A. et al. Bacteria that inhibit quorum sensing decrease biofilm formation and virulence in *Pseudomonas aeruginosa* PAO1. *Pathog. Dis.* **70**, 271–279. <https://doi.org/10.1111/2049-632X.12124> (2014).
50. Huang, X. et al. *Acinetobacter venetianus*, a potential pathogen of red leg disease in freshwater-cultured whiteleg shrimp *Penaeus vannamei*. *Aquac. Rep.* **18**, 100543. <https://doi.org/10.1016/j.aqrep.2020.100543> (2020).
51. Hong, X., Lu, L. & Xu, D. Progress in research on acute hepatopancreatic necrosis disease (AHPND). *Aquac. Int.* **24**, 577–593. <https://doi.org/10.1007/s10499-015-9948-x> (2016).
52. Sarmiento-Ramírez, J. M., van der Voort, M., Raaijmakers, J. M. & Diéguez-Uribeondo, J. Unravelling the microbiome of eggs of the endangered sea turtle *Eretmochelys imbricata* identifies bacteria with activity against the emerging pathogen *Fusarium falciforme*. *PLoS ONE* **9**, e95206. <https://doi.org/10.1371/journal.pone.0095206> (2014).
53. Ninawe, A. S. & Selvin, J. Probiotics in shrimp aquaculture: Avenues and challenges. *Crit. Rev. Microbiol.* **35**, 43–66. <https://doi.org/10.1080/10408410802667202> (2009).
54. Babić, M. N., Zupančič, J., Gunde-Cimerman, N. & Zalar, P. Yeast in anthropogenic and polluted environments. In *Yeasts in Natural Ecosystems: Diversity* (eds. Buzzini, P., Lachance, M. A. & Yurkov, A.) 145–169 (Springer, 2017).
55. Lee, C. T. et al. The opportunistic marine pathogen *Vibrio parahaemolyticus* becomes virulent by acquiring a plasmid that expresses a deadly toxin. *Proc. Natl. Acad. Sci. USA* **112**, 10798–10803. <https://doi.org/10.1073/pnas.1503129112> (2015).
56. Ooi, M. C., Goulden, E. F., Trotter, A. J., Smith, G. G. & Bridle, A. R. *Aquimarina* sp. associated with a cuticular disease of cultured larval Palinurid and Scyllarid lobsters. *Front. Microbiol.* **11**, 573588. <https://doi.org/10.3389/fmicb.2020.573588> (2020).
57. Zheng, Y. et al. *Aquimarina hainanensis* sp. nov., isolated from diseased Pacific white shrimp *Litopenaeus vannamei* larvae. *Int. J. Syst. Evol. Microbiol.* **66**, 70–75. <https://doi.org/10.1099/ijsem.0.000675> (2016).
58. Xiong, J. et al. Quantitative prediction of shrimp disease incidence via the profile of gut eukaryotic microbiota. *Appl. Microbiol. Biotechnol.* **102**, 3315–3326. <https://doi.org/10.1007/s00253-018-8874-z> (2018).
59. Vargas-Albores, F. et al. Bacterial biota of shrimp intestine is significantly modified by the use of a probiotic mixture: A high throughput sequencing approach. *Helgol. Mar. Res.* **71**, 5. <https://doi.org/10.1186/s10152-017-0485-z> (2017).
60. Berg, G. et al. Microbiome definition re-visited: Old concepts and new challenges. *Microbiome* **8**, 103. <https://doi.org/10.1186/s40168-020-00875-0> (2020).
61. Dai, W., Qiu, Q., Chen, J. & Xiong, J. Gut eukaryotic disease-discriminatory taxa are indicative of Pacific white shrimp (*Litopenaeus vannamei*) white feces syndrome. *Aquaculture* **506**, 154–160. <https://doi.org/10.1016/j.aquaculture.2019.03.034> (2019).
62. Deusch, S. et al. A structural and functional elucidation of the rumen microbiome influenced by various diets and microenvironments. *Front. Microbiol.* **8**, 1605. <https://doi.org/10.3389/fmicb.2017.01605> (2017).
63. Ning, M. et al. Proteomic and metabolomic responses in hepatopancreas of whiteleg shrimp *Litopenaeus vannamei* infected by microsporidian *Enterocytozoon hepatopenaei*. *Fish Shellfish Immunol.* **87**, 534–545. <https://doi.org/10.1016/j.fsi.2019.01.051> (2019).
64. Kanehisa, M. & Goto, S. KEGG: Kyoto encyclopedia of genes and genomes. *Nucleic Acids Res.* **28**, 27–30. <https://doi.org/10.1093/nar/28.1.27> (2000).

Acknowledgements

The authors would like to thank Paul Schofield and Tanner Padilla for their support with EHP experimental challenge and Tiffany Bledsoe for her assistance with histology and scanning of slides.

Author contributions

R.C.F. and A.K.D. conceived this project, designed the experiments and edited all versions of the manuscript. R.C.F. performed histopathology, in situ hybridization and nucleic acid extractions. J.A.L.C. analyzed the NGS data, assign infection grades of the organisms using quantitative histology, created Biorender illustrations and wrote the manuscript. All authors commented during manuscript revision.

Funding

Funding for this research was provided by the College of Agriculture & Life Sciences, University of Arizona to Arun K. Dhar. Partial funding was provided by the Aquaculture Pathology Laboratory Disease Diagnostic Fund.

Competing interests

The authors declare no competing interests.

Additional information

Correspondence and requests for materials should be addressed to A.K.D.

Reprints and permissions information is available at www.nature.com/reprints.

Publisher's note Springer Nature remains neutral with regard to jurisdictional claims in published maps and institutional affiliations.



Open Access This article is licensed under a Creative Commons Attribution 4.0 International License, which permits use, sharing, adaptation, distribution and reproduction in any medium or format, as long as you give appropriate credit to the original author(s) and the source, provide a link to the Creative Commons licence, and indicate if changes were made. The images or other third party material in this article are included in the article's Creative Commons licence, unless indicated otherwise in a credit line to the material. If material is not included in the article's Creative Commons licence and your intended use is not permitted by statutory regulation or exceeds the permitted use, you will need to obtain permission directly from the copyright holder. To view a copy of this licence, visit <http://creativecommons.org/licenses/by/4.0/>.

© The Author(s) 2022